

---

---

METHODS  
OF PHYSICAL EXPERIMENT

---

---

## Locating the Neutrino Interaction Vertex with the Help of Electronic Detectors in the OPERA Experiment

Yu. A. Gornushkin\*\*\*, S. G. Dmitrievsky\*\*, and A. V. Chukanov\*

*Joint Institute for Nuclear Research, Dubna, 141980 Russia*

\*chukanov@jinr.ru

\*\*dmitr@jinr.ru

\*\*\*gornushk@yandex.ru

**Abstract**—The OPERA experiment is designed for the direct observation of the appearance of  $\nu_\tau$  from  $\nu_\mu \rightarrow \nu_\tau$  oscillation in a  $\nu_\mu$  beam. A description of the procedure of neutrino interaction vertex localization (Brick Finding) by electronic detectors of a hybrid OPERA setup is presented. The procedure includes muon track and hadronic shower axis reconstruction and a determination of the target bricks with the highest probability to contain the vertex.

DOI: 10.1134/S1547477115010100

### INTRODUCTION

The OPERA experiment [1, 2] is designed to detect  $\nu_\mu \rightarrow \nu_\tau$  oscillations in direct  $\nu_\tau$  appearance mode in an initially pure muon neutrino beam produced at CERN. The OPERA detector [3] is located at the Gran Sasso underground laboratory in Italy, 730 km away from the accelerator in Geneva (Switzerland), making it possible to detect tau neutrino interactions with high signal-to-background ratio. The  $\nu_\mu \rightarrow \nu_\tau$  oscillations are considered responsible for the deficit of muon neutrinos in atmospheric showers [4], and the experimental verification of this transition is a requisite for the mixing model of three-component neutrinos. The OPERA experiment registers  $\tau$  neutrinos via a charged current channel through direct observation of a short-lived  $\tau$  lepton appearing in the a primary neutron interaction vertex. Therefore, the requirements imposed on the detector are hardly compatible: it should have large mass to increase the neutrino events statistics and, at the same time, good spatial resolution for tau-lepton recognition. To solve this problem, the OPERA experiment uses a hybrid detector (see Fig. 1), which includes electronic detectors (target tracker (TT), magnetic spectrometers) and a target area having a modular structure and consisting of 150000 bricks arranged into walls with total mass of 1250 t. Each brick of size  $12 \times 10 \times 7.5$  cm is a set of 56 lead plates 1 mm thick (target) alternating with 57 plates of nuclear photoemulsion, which permits one to get the micron spatial resolution necessary for tau-lepton observation.

Data analysis in the experiment is performed in two stages: the target brick where neutrino interac-

tion occurred is located based on information from the electronic detectors, and then this brick is extracted to search for the tracks and vertex of the event, as well as for the elaborate study of the interaction characteristics. The great majority of the detected neutrino events result from the interaction of muon neutrinos with the detector material through the charged ( $\nu_\mu + N \rightarrow \mu^- + X$ ) and neutral ( $\nu_\mu + N \rightarrow \nu_\mu + X$ ) current channels (CC and NC). The target brick where such an event occurred is located using the electronic detectors, following which a comprehensive analysis of the topology of the event in the emulsion allows us to identify tau-neutrino interactions appearing as a small admixture as a result of oscillations in the beam. The search for a vertex, i.e., identification of the target brick containing the neutrino interaction vertex, through an analysis of data from the electronic detectors, is an important task of experimental data processing [5–10]. More accurate and efficient localization permits one to reduce the amount of information in the photoemulsion to be analysed (the most time-consuming part of experimental data processing) and slow down the reduction of the target mass in the detector with time (the target bricks are not replaced after extraction and analysis).

In the present paper we consider in more detail the methods used for event analysis using the OPERA electronic detectors, show the results of evaluating the efficiency of finding the vertex, and describe the EventViewer graphical shell used for the display of electronic-detector data and for the visual control of event processing.

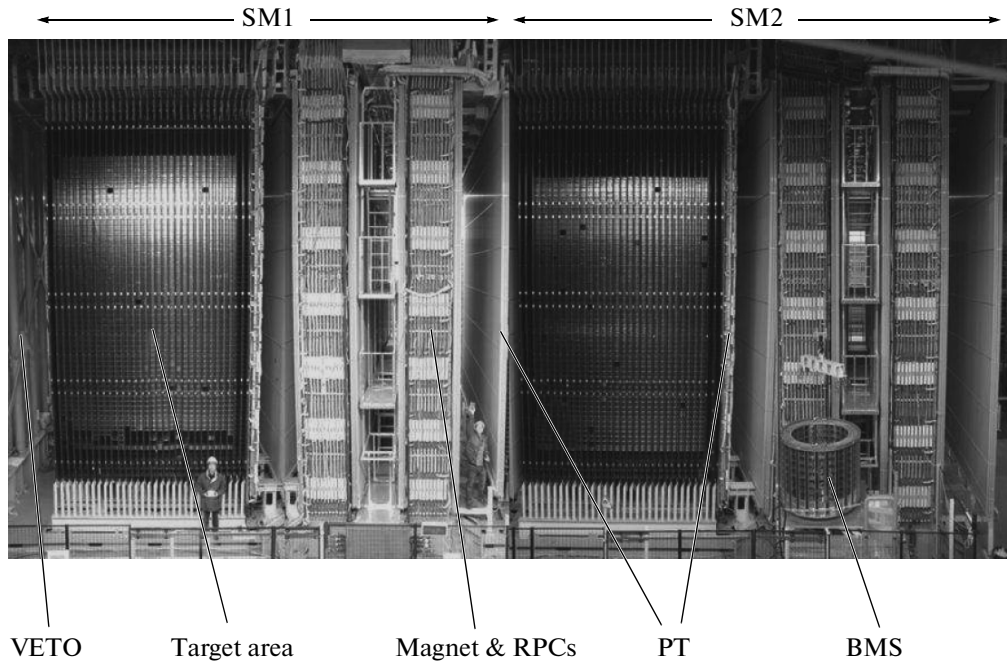


**Fig. 1.** General view of the OPERA detector: two identical supermodules (SM1 and SM2), each including the target area, magnet, and a system of resistive plane chambers (RPC) and drift tubes (PT). The target area contains  $\sim 75\,000$  bricks located between the planes of the TT. The VETO system is used for selecting neutrino events with origins inside the target area. The extraction of the bricks from the detector is done with a BMS robot.

## 1. ANALYSIS OF ELECTRONIC-DETECTOR DATA FOR LOCATING THE NEUTRINO INTERACTION VERTEX

The major task of analysis of electronic-detector data in the OPERA experiment is locating the neutrino interaction vertex. Taking into account the modular structure of the OPERA target area, consisting of lead-emulsion bricks, as well as the relatively low spatial resolution of the electronic track detectors, the initial goal of the vertex search is to identify a brick where a neutrino interaction occurred. After the successful selection of the brick, the interaction vertex search is further performed making use of emulsion analysis techniques. Electronic-detector data processing for vertex localization includes the following stages:

- (1) Primary processing electronic-detector signals received when registering a neutrino event, which includes the suppression of background hits and a calculation of energy released from detector calibration (see 1.1 and 1.2);
- (2) Reconstruction of muon track and hadronic shower axis (see 1.3 and 1.4);
- (3) Determination of the target walls with the highest probability of containing the interaction vertex (see 1.5);
- (4) Calculation of probability for finding the vertex in bricks from the selected walls (see 1.6).

### 1.1. Calculation of Energy Deposit in TT

The TT [11] consists of 62 planes and has a modular structure. Each plane consists of eight modules

which measure  $X$  and  $Y$  coordinates. Each TT module is constituted of 64 scintillator strips of size  $26 \times 10 \times 6860$  mm. Before assembly, all TT strips were calibrated by 2 MeV electrons from a  $^{90}\text{Sr}$   $\beta$  radioactive source, imitating the passage of a minimum ionizing particle (MIP), which loses on average an energy of  $E_{MIP} = 2.15$  MeV when crossing a 1-cm plastic scintillator. Nine points evenly distributed along each strip were under irradiation; the amplitude of a signal ( $E_{left}$ ,  $E_{right}$ ) was registered from both sides of the wave length-shifting fiber by which the scintillation light is captured and carried over to the multichannel photomultipliers placed on both sides of the module. The light propagating along the fiber is partially absorbed; therefore, the amplitude at the right and at the left depend on the source location along the strip. The dependences derived in this way for every strip were approximated by a following signal attenuation function (see Fig. 2):

$$\begin{cases} E_{left} = E_0 \left[ \alpha e^{-\frac{x}{\lambda_s}} + (1 - \alpha) e^{-\frac{x}{\lambda_l}} \right], \\ E_{right} = \beta E_0 \left[ \alpha e^{-\frac{L_0 - x}{\lambda_s}} + (1 - \alpha) e^{-\frac{L_0 - x}{\lambda_l}} \right], \end{cases}$$

where  $x$  is the distance from the irradiation point to the left photomultiplier, where the origin is,  $E_0$  is the num-

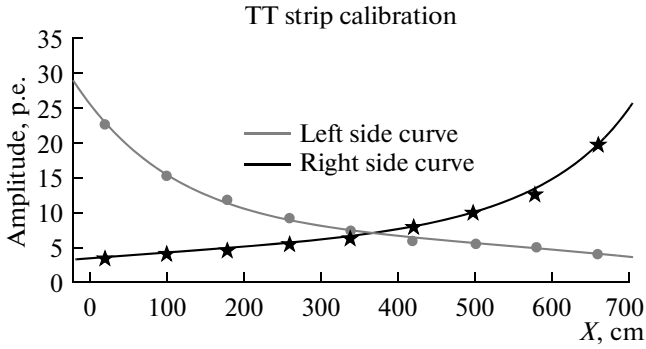


**Fig. 2.** Amplitude of a signal in the TT strip in relation to the distance from the location of a passing particle to PMTs placed at both ends.

ber of PMT photoelectrons at  $x = 0$ ,  $\lambda_s$  is the “short” attenuation length,  $\lambda_l$  is the “long” attenuation length,  $\alpha \in (0, 1)$  is the coefficient characterizing the contribution of each exponent to signal attenuation,  $\beta$  is the quality coefficient that takes into account a possible difference between the optical contacts on the left and right PMT, and  $L_0$  is the strip length.

Using this calibration, the energy deposited in the strip when a minimum ionizing particle passes through it can be estimated as

$$E^{rec} = \frac{E_{MIP}(E_{left}^{rec} + E_{right}^{rec})}{2E_0},$$

where  $E_{left}^{rec} = \frac{E_{left}}{\left[ \alpha e^{-\frac{x}{\lambda_s}} + (1-\alpha)e^{-\frac{x}{\lambda_l}} \right]}$  and  $E_{right}^{rec} = \frac{E_{right}}{\left[ \alpha e^{-\frac{L_0-x}{\lambda_s}} + (1-\alpha)e^{-\frac{L_0-x}{\lambda_l}} \right]}$ .

The reconstructed energy deposit is used later on in the procedures of hadron shower axis reconstruction and determination of a target wall containing the interaction vertex (see 1.5).

### 1.2. Event Filtering

Track information is most essential for searching for the interaction vertex. However, the event may contain isolated signals (or isolated signal groups) resulting from the interaction of neutral particles (neutrons and gamma quanta) with the material in the detector, noise, and cross talks in the neighboring channels of the photomultiplier. To facilitate the track reconstruction, some preliminary event filtering based on the *cellular automaton* approach [12] is performed to suppress the isolated TT fits. For this purpose, two rectangles nested into each other, forming the internal

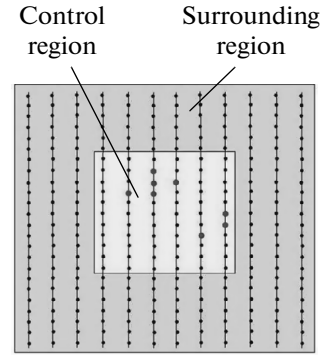


**Fig. 3.** Principle of filtering isolated fits (or groups of fits) in the TT.

(control) and external (surrounding) regions where the number of fits is counted up, move step by step in every projection throughout the event (see Fig. 3). If at a certain iteration there was no hit in the external region and at the same time the number of hits in the internal region turned out to be under the critical value, then such a group of fits is considered isolated and is removed (provided that this group does not make the most of the event). A smooth variation of the sizes of the rectangles and their respective critical values allows one to reduce the number of isolated hits (or small groups of hits), which may distort the topology of events. One example of an OPERA event before and after filtering is shown in Fig. 4. Monte Carlo studies using Geant3 [13], which took into account the factors leading to the appearance of single hits (including cross talks in PMT channels), have shown that the application of the described filtering procedure leaves the efficiency of finding the muon track unchanged, accelerating the process of their reconstruction. In addition, the filtering helps us better locate the target wall containing the neutrino interaction vertex (see 1.5).

### 1.3. Muon-Track Reconstruction

Reconstruction of the muon track in neutrino events, occurring via the CC and  $\tau \rightarrow \mu$  channel, is an important step in looking for the target brick where the neutrino interaction occurred, since the muon usually travels a long distance in the detector; its track shows up clearly and indicates the direction to the event vertex.

The reconstruction of other particle tracks in the event is almost always difficult, especially in the area of hadron-shower development, as the spatial resolution of TT in the OPERA detector (about 7.5 mm) in the general case does not allow us to distinguish individual tracks near the interaction vertex.

Tracks in the electronic detectors are reconstructed using several algorithms.

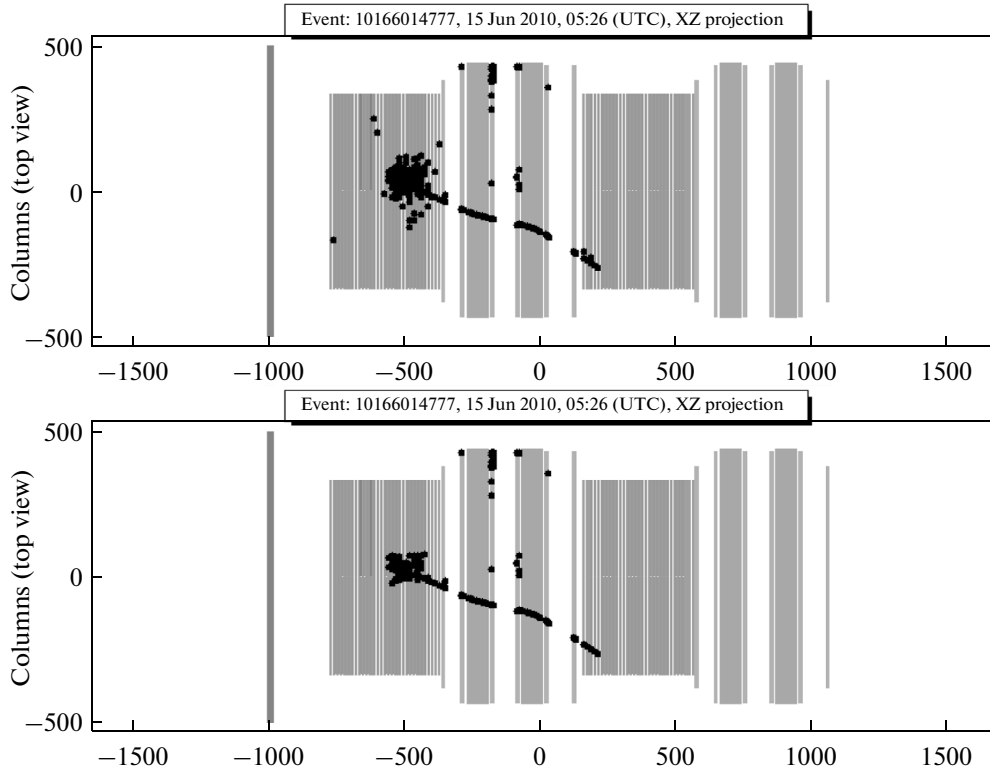


Fig. 4. View of an OPERA event before (top) and after (bottom) filtering.

(1) Hough transform for reconstructing straight tracks

*Hough transform* [14] is an efficient pattern-recognition method which is widely used in experimental physics for track reconstruction. The Hough linear transform uses a representation of a straight line on a plane in the form  $x\cos\theta + y\sin\theta = \rho$ .

This equation determines the line passing through the point  $(x, y)$  and perpendicular to the straight-line segment drawn from the point  $(0, 0)$  to the point  $(\rho, \theta)$  in polar coordinates (see Fig. 5).

For every existing point  $(x_i, y_i)$ , values of the angle  $\theta_j$  are exhausted with a given step in the interval from 0 to  $2\pi$  and the respective  $\rho_{ij}$  values are calculated by the formula. The points  $(\rho_{ij}, \theta_j)$  are stored into a two-dimensional histogram. If there are straight-line tracks

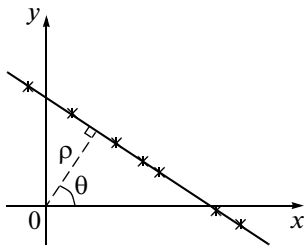


Fig. 5. Straight line  $x\cos\theta + y\sin\theta = \rho$ .

in the event, then this histogram will contain distinct peaks because, for the points lying on the same straight line,  $\rho$  and  $\theta$  are constants. The parameters of the  $k$ th track lying on the straight line  $y = A_kx + B_k$  are determined from the center of gravity of the corresponding peak  $(\rho_k, \theta_k)$  like

$$A_k = -\frac{1}{\tan\theta_k}, \quad B_k = \frac{\rho_k}{\sin\theta_k}.$$

An example of using the Hough transform for muon-track reconstruction in the CC  $\nu_\mu$  event is given in Fig. 6. The track parameters were determined according to the main peak in the two-dimensional histogram shown in Fig. 7.

(2) Track-tracing method

Not all muon tracks are straight because of multiple scattering. The presence of a strong hadron shower in the vicinity of the interaction vertex may significantly complicate the observation of distinct peaks in the space of the parameters  $(\rho, \theta)$ . In these cases it is more efficient to begin muon-track recognition at the end of the event (where there are no signals from the shower particles). For this purpose, a *tracing method* is used which works according to the following iterative scheme:

(a) the choice of search direction in a given step. This is usually a linear approximation of the last seven hits found on the track;

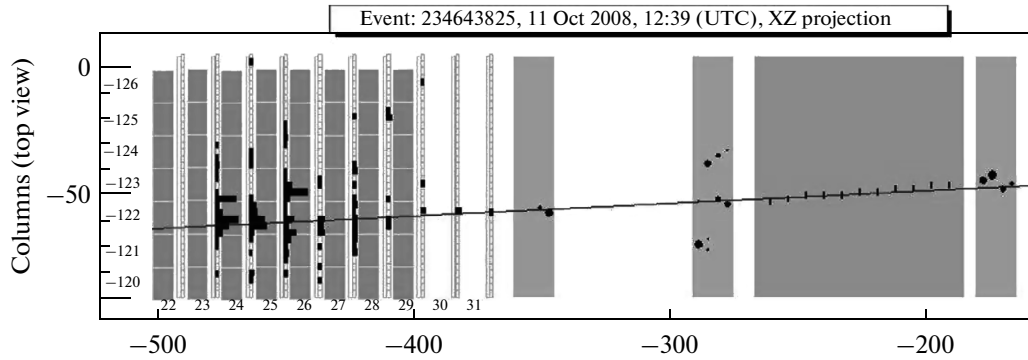


Fig. 6. Muon track found with the help of the Hough transform.

(b) the search for fits in the subsequent planes of the detector in a predetermined angular range. The angular range for the search is chosen according to the spatial resolution of the electronic detectors (TT, resistive plane chambers, or drift tubes). The operation efficiency of a particular detector and the relative positions of different types of detectors (setup geometry) are also taken into account. When several hits are within the selected angular range, the one nearest to the predicted particle trajectory is chosen;

(c) Inclusion of the found fit in the track and continuation of the iterative search procedure from step (a), or the cessation of further searching if no fit was found in a succession of planes of the detector.

Note that, as a permissible track variation from a straight line in consistent coordinate planes, the described track recognition procedure based on the tracing method uses not a multiple scattering estimate, but a coordinate measuring step, being of a larger magnitude.

After track recognition and the selection of its hits, the direction of the track is refined in the vicinity of the event vertex. To do this, the straight-line approximation of 14 points is performed on the track in the TT planes where the density of hits near the track is small enough, since, upon the operation of a succession of TT strips (for instance, in the region where a hadron shower is registered), these hits cannot be used for track approximation. If the event occurred at the end of a supermodule, then the approximation also includes signals from the detectors belonging to magnetic spectrometers.

All bricks of the target in OPERA are equipped with an external interface: two emulsion plates in an independent cassette which serve to verify predictions of the electronic detectors. A complete analysis of each extracted brick is performed only if converging tracks are observed in its external layers, or at least one of the tracks has a continuation in the electronic detectors. The relative position of the target walls and TT planes is taken into account as well.

Figure 8 shows results of a comparison of the parameters (location and slope) of the muon tracks reconstructed in the electronic detectors with those of the tracks observed in the external interface emulsion.

The root-mean-square deviation of track position from the predicted value is close to the theoretical limit of the TT resolution ( $\sim 7.5$  mm), suggesting a good geometrical calibration of the detectors and high-quality track reconstruction.

#### 1.4. Hadron Shower Axis Reconstruction

Muon-track reconstruction most effectively helps find the vertex of an event, but in many cases, e.g., HT channel interaction, there may not be distinct tracks in the event at all. In these cases one performs a reconstruction of the hadron shower axis, which should point to the vertex on the assumption that the shower develops symmetrically relative to the axis.

A robust line-fitting method is used to reconstruct the hadron shower axis [15]. The idea of this method consists of the modification of a functional, which is minimized in the *least-square method (LSM)* so that

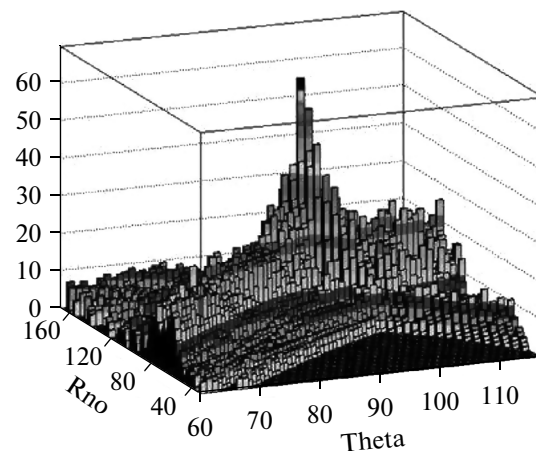
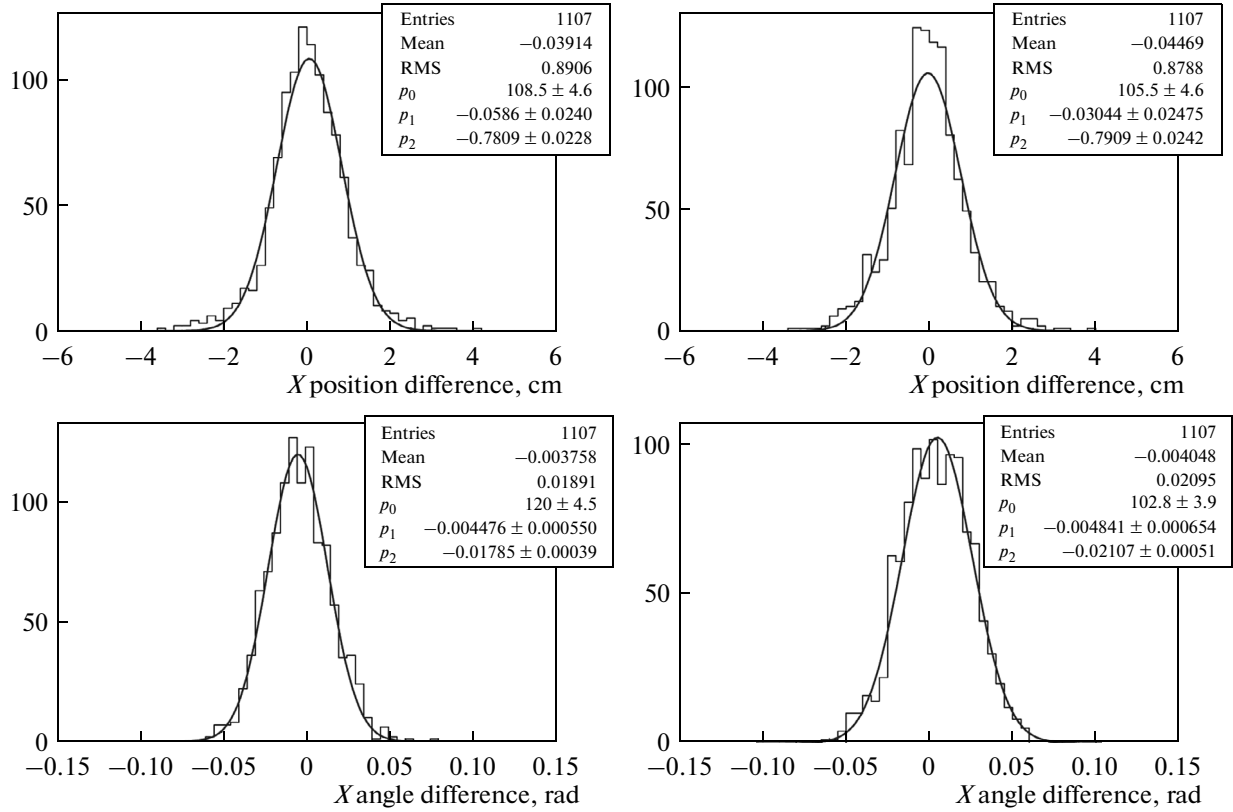


Fig. 7. Histogram of an event in the space of the parameters  $\rho$  and  $\theta$ .



**Fig. 8.** Comparison of the parameters of the tracks reconstructed in the electronic detectors and observed in the external interface emulsion.

the minimization gives a robust (efficient) estimate in terms of non-Gaussian errors and in the presence of points away from the fitting line:

$$L_{LSM}(p) = \sum_i \varepsilon_i^2 \rightarrow L_{rob.}(p) = \sum_i \rho(\varepsilon_i).$$

Here,  $p$  is the vector of free parameters,  $\varepsilon_i$  is the distance from the  $i$ th point to the fitting line, and  $\rho(\varepsilon)$  is a rapidly converging function.

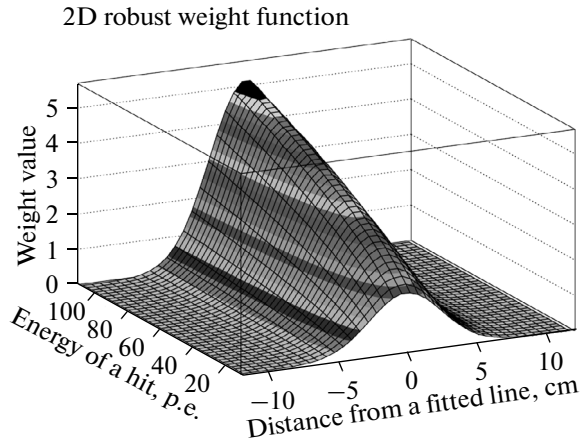


**Fig. 9.** View of the weight function used for reconstructing the hadron-shower axis.

The values of the free parameters are determined from the equation

$$\frac{\partial L(p)}{\partial p} = \sum_i w(\varepsilon_i) \frac{\partial \varepsilon_i}{\partial p} \varepsilon_i = 0,$$

which is similar to the conventional LSM equation, but instead of numeric multiplier it contains a weight function

$$w(\varepsilon) = \frac{1}{\varepsilon} \frac{\partial \rho(\varepsilon)}{\partial \varepsilon}.$$

Therefore, every measured point acquires its own weight. At first, the weights of all points are taken equal to unity, and then they are recalculated before every subsequent iteration, until the values of the free parameters cease to change (i.e., the procedure converges due to the fact that the points whose weights become negligibly small are ignored).

In our case, after testing on a sampling of simulated events, we chose the following as a weight function:

$$w(E, \varepsilon, \sigma) = \sqrt{E} \exp\left(-\frac{\varepsilon^2}{\sigma^2}\right),$$

which depends on the hit energy  $E$  and the hit distance to the current position of the axis. Figure 9 shows a typical example of this function. The parameter  $\sigma$

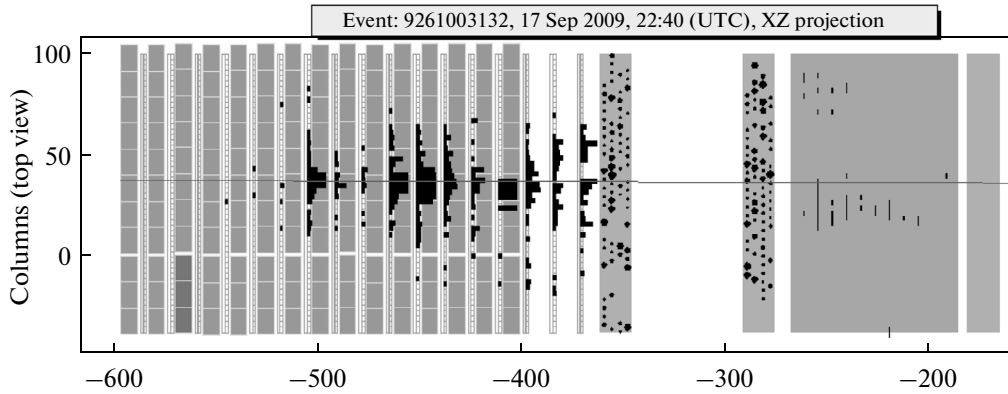


Fig. 10. Example of reconstruction of the hadron-shower axis.

gradually decreases in the course of the iteration procedure.

To locate the hadron shower axis, we used fits in the first five planes of the event, except for those belonging to the muon track. A straight line parallel to the  $Z$  axis and passing through the center of gravity of the event was chosen as an initial approximation.

An example of reconstruction of a hadron-shower is shown in Fig. 10.

We have tested other methods of shower axis reconstruction as well, in particular, the method of line-fitting over the centers of gravity of the energy released in every plane of TT, but all these techniques showed smaller reconstruction efficiency of the direction to the interaction vertex when compared with the described method of robust fitting. Distributions of deviations of the reconstructed shower axis from the event vertex for three options of reconstruction are given in Fig. 11 for comparison: (1) with the use of LSM, (2) with center-of-gravity approximation in the TT planes, and (3) with robust approximation.

### 1.5. Determination of the Interaction Vertex Wall

The difficulty of determining the target wall containing a brick in which a neutrino interaction occurred is mainly due to the presence of particles escaping to the backward hemisphere (against the direction of the beam). These particles produce signals in the TT planes located upstream the vertex brick, significantly blurring the search area. Simulated distributions of probability of vertex location in the  $k$ th wall relative to the first (in beam) TT planes having hits belonging to the given event are shown as an example in Table 1.

In the analysis of OPERA experimental data, the wall determination is performed in two steps:

(1) preliminary selection of TT planes.

Along with the event-filtering procedure described above, three TT planes, beginning with the number  $s$ , are selected at this step for further analysis (here, as

above, the event is considered to begin in the wall with the number 1 and the vertex is located in the wall with the number  $k$  starting from the following conditions:

(i) The planes with the numbers  $s$  and  $s + 1$  contain fits in both projections;

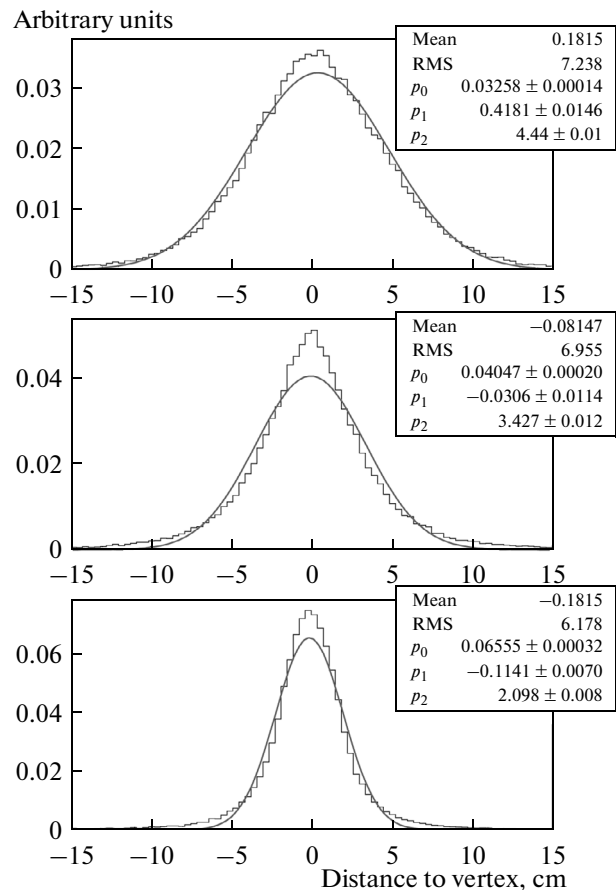


Fig. 11. Deviation of the reconstructed hadron-shower axis from the event vertex for (top) LSM, (middle) energy-release centers approximation in the TT planes, and (bottom) robust approximation.

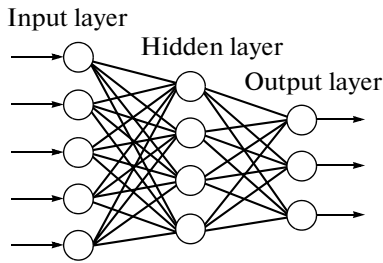


Fig. 12. Structure of an MLP with one hidden layer.

(ii) The total energy release registered in each of the planes with the numbers  $s$  and  $s + 1$  exceeds two photoelectrons.

In Table 2 it is shown that after this step the number  $k$  of the wall with vertex in most events (99.0% for CC and 94.6% for NC channel) falls within the interval  $[s; s + 2]$ . Therefore, three TT planes with these numbers are selected for the second step.

(2) Estimation of probabilities for a vertex to be found in all three target walls.

The data from three preselected TT planes is analyzed with the help of an *artificial neural network (ANN)*, namely, a *multilayer perceptron (MLP)* [16]. In high-energy physics, an MLP is often useful in multi-parameter problems of classification due to the possibility of teaching these ANNs on bulks of Monte Carlo simulated events.

The point structure of the MLP presented in Fig. 12 includes three layers of unit computational cells (artificial neurons): input, hidden, and output. Each subsequent layer interacts with the previous one

by means of weight links between the neurons. The MLP input vector of the characteristics of the studied object passes through the network and transforms into a vector characterizing the extent to which the given object belongs to one or another class. The MLP is tuned by the backward propagation of error for a large sample of training data where the class of each object is known in advance from the model or defined in any other way.

Nineteen variables describing the geometrical distribution and amplitudes of signals from the electronic detectors in the given event (their total number, the distance to the hadron shower axis, and the scatter relative to the energy-weighted average value), as well as the ratio energy released in the first three selected TT planes, are used as input parameters for ANN.

MLP training was done on a sample of  $\sim 100000$  simulated  $\nu_\mu$  CC and NC events (ratio CC/NC = 3/1). The energy functional was minimized by the conjugate gradient method [17]. At the output, the neural network yields three probabilities for target walls selected at step 1 to contain the neutrino interaction vertex.

For a quality check of the ANN used in the problem of the vertex localization problem, its efficiency was compared with that of two other classifiers, namely, the ANN of a similar structure from the Stuttgart neural network simulator (SNNS) [18] and an algorithm based on the boosted decision tree (BDT) [19]. The results of comparison [9] showed that the employed neural network is more suitable for solving the selected task than the BDT algorithm and its efficiency is almost the same as that of the MLP of the SNNS package.

Table 1. Position of the wall with vertex relative to the initial wall of the event (for the simulated data)

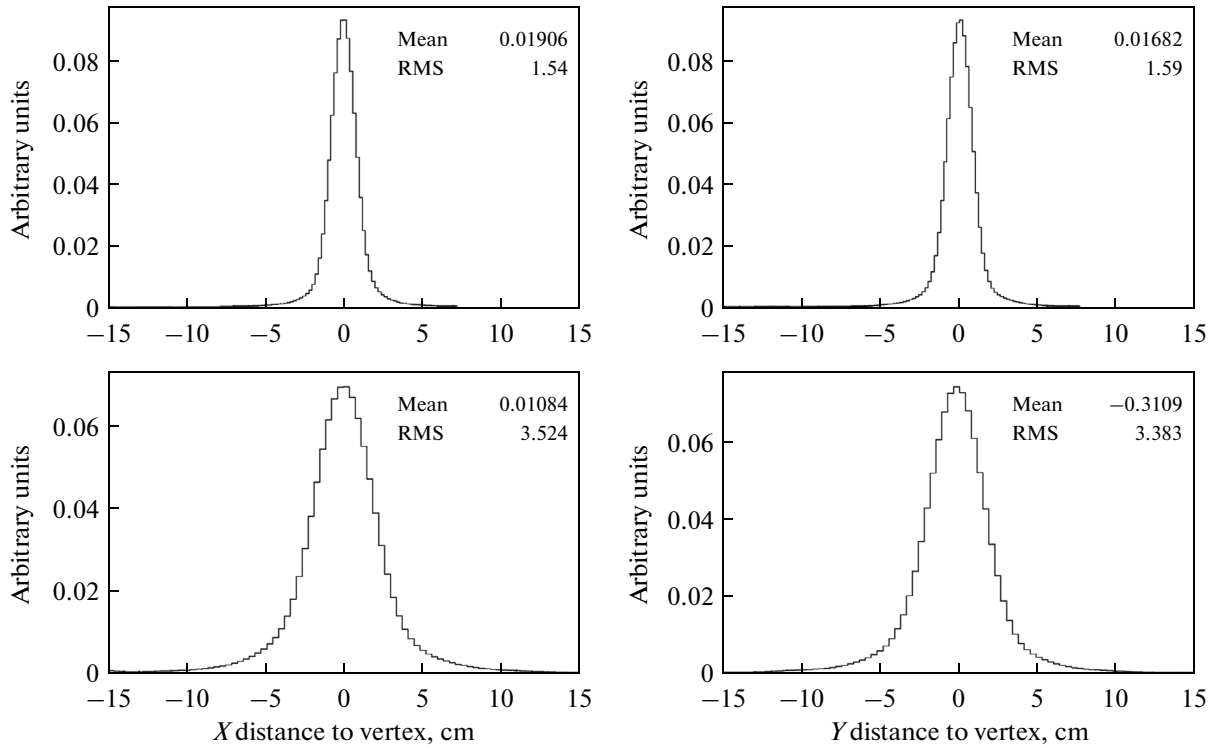
	$k < 1$	$k = 1$	$k = 2$	$k = 3$	$k > 3$
For CC channel:	0.0%	40.7%	27.5%	12.3%	19.4%
For NC channel:	1.0%	38.7%	27.6%	12.7%	20.0%

Table 2. Position of the wall with vertex relative to the selected wall (for the simulated data)

	$k < s$	$k = s$	$k = s + 1$	$k = s + 2$	$k > s + 2$
For CC channel:	0.6%	80.5%	17.3%	1.2%	0.4%
For NC channel:	5.0%	76.0%	17.5%	1.0%	0.4%

### 1.6. Prediction of Brick with Interaction Vertex

After the reconstruction of the muon track or the hadron-shower axis, their parameters are used to determine the target bricks with highest probability to contain the event vertex. In this case the results of ANN application are also useful for determining the relative probability of vertex location in the target wall. The relative probability of vertex location in the target



**Fig. 13.** Muon-momentum- and shower-energy-averaged distributions of the distance from the neutrino event vertex to the muon track (top) and to the hadron-shower axis (bottom) in the XZ (left) and YZ (right) projection.

brick is calculated by the formula  $P_{brick} = P_{wall}P_xP_y$ , where

$$P_t = \int_{t_1 z_1}^{t_2 z_2} \rho_t(t, z)(dt)dz \quad (t = x, y).$$

Here, the coordinates  $x_1, y_1, z_1$  and  $x_2, y_2, z_2$  define the volume occupied by the brick in space;  $\rho_x$  is the density of probability of the track passing through the point  $(x, z)$  determined from the error in the measurement of the track parameters and the distance to this point. The  $\rho_x$ , as well as probability density  $\rho_y$ , was derived by simulating the registration of neutrino events in the detector for different muon momenta and hadron shower energy (see Fig. 13).

The interaction vertex localization efficiency  $\varepsilon_{BF}$  in relation to the maximum number of extracted target bricks was estimated by simulation. Table 3 presents the results of this estimation for different samples: 5000 CC  $\nu_\mu$  events and 5000 NC  $\nu_\mu$  events, as well as for a mixed sample of 13800 CC, NC and quasi-elastic (QE) interaction ( $\nu_\mu + n \rightarrow \mu^- + p$ ) events.

## 2. EVENTVIEWER GRAPHICAL SHELL

For visual control of data processing, the EventViewer graphical shell has been developed, which is a convenient and easily adjustable interface with a set of necessary functions, settings, and tools for viewing

and analyzing both real and simulated events. The main program window with an image of one of the OPERA events detected in 2010 is shown in Fig. 14.

The useful features of the program include the graphical representation of a specified event, wide-ranging scaling of the event area (from a few  $\text{cm}^2$  to the size of the entire detector), and saving an image of the event in a selected file format. EventViewer also allows one to turn on and off various options of event reconstruction in the interactive mode (filtering, reconstruction of muon track or shower axis, setting the TT initial plane to be presented to ANN, etc.), perform the straight-line approximation of tracks by the fits selected by the user, project the tracks found in the emulsion into the area of electronic detectors (see Fig. 15), etc.

**Table 3.** Efficiency of vertex location for the simulated events

Number of extr. bricks	$\varepsilon_{BF}$ , CC	$\varepsilon_{BF}$ , NC	$\varepsilon_{BF}$ , CC/NC/QE
1 brick	77.5%	58.5%	74.1%
2 bricks	91.3%	75.4%	88.0%
3 bricks	94.8%	82.3%	92.2%
4 bricks	96.7%	86.1%	94.4%

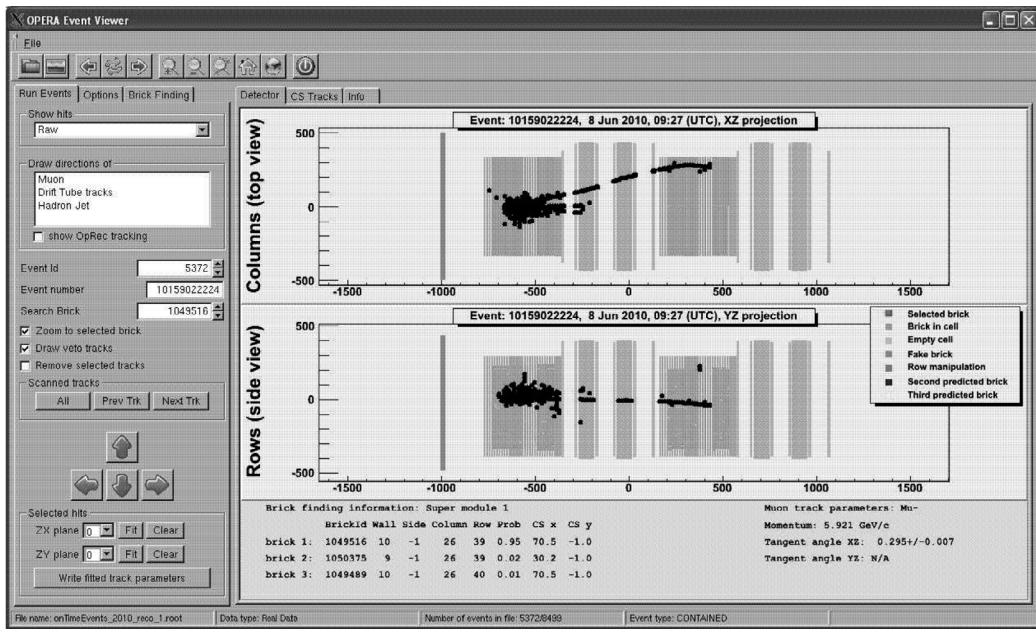


Fig. 14. View of an OPERA event in the EventViewer main window.

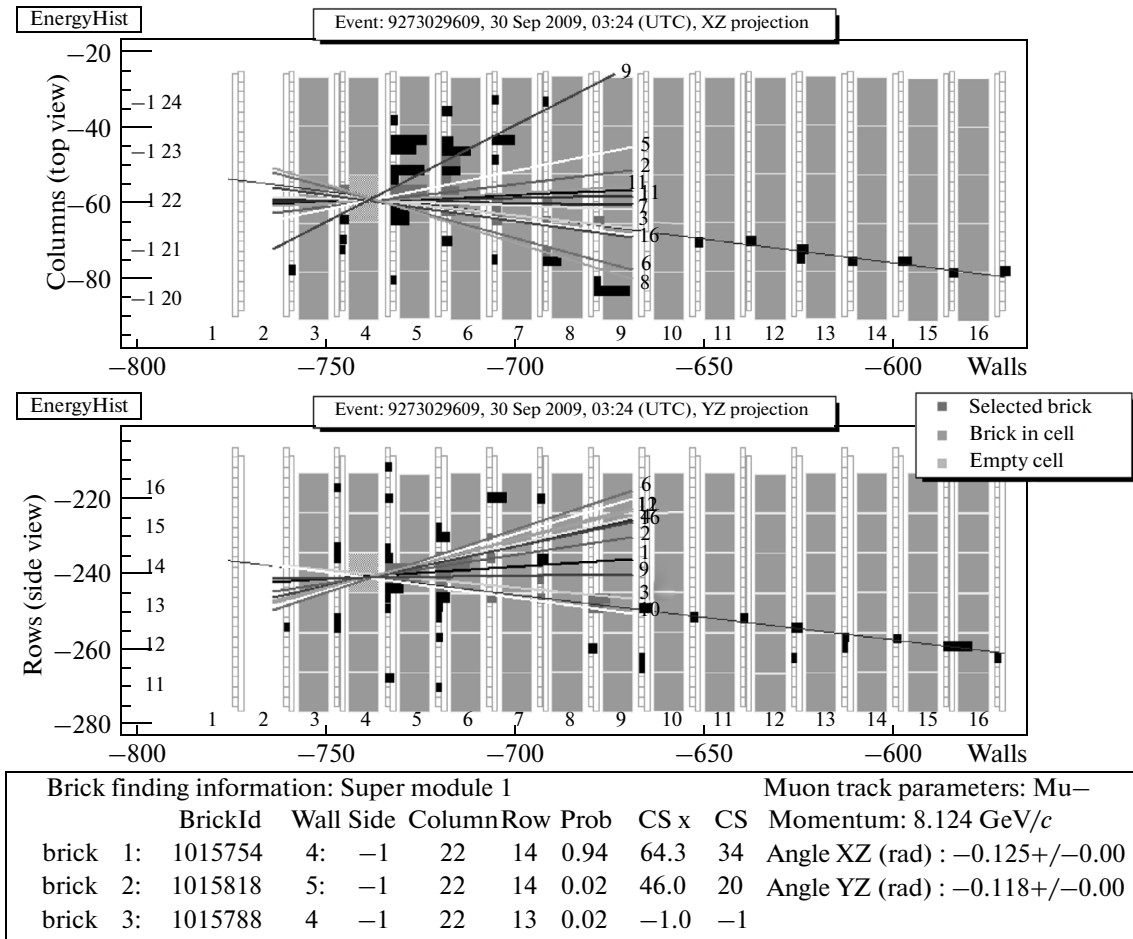


Fig. 15. Projection of tracks found in photoemulsion into the TT area.

## CONCLUSIONS

A procedure for determining the target brick containing the interaction vertex from the data of OPERA electronic detectors has been described in the present work. Modern data-analysis methods used for processing neutrino events allow a 65% efficiency of interaction vertex location in the most probable brick. A further gain in efficiency is reached by searching for the vertex in the next probable bricks. All the algorithms are implemented in C++ with OpBrickFinder open-source code, which is integrated into the OPERA software. In 2009 this program was used to analyze 40% of the OPERA events and demonstrated highly efficient and fast data processing. OpBrickFinder has been used to analyze all experimental data since 2010. The program consists of several autonomous modules which, upon appropriate adaptation and tuning, can be applied to the data processing of other experiments.

## ACKNOWLEDGMENTS

We thank A. Krasnoperov, G. Ososkov, and A. Stadnik for useful discussions, as well as A. Ariga, F. Di Capua, A. Cazes, D. Duchesneau, T. Ferber, T. Le Fleur, I. Kreslo, G. De Lellis, P. Migliozzi, Y. Nonoyama, O. Sato, and B. Wonsak for their useful contributions and remarks. This work was supported by the Russian Foundation for Basic Research, (project 12-02-12142-ofi\_m), as well as by grants for young scientists and specialists of the Joint Institute for Nuclear Research, projects 13-201-02 and 14-202-04.

## REFERENCES

1. M. Guler et al. (OPERA Collaboration), "An appearance experiment to search for  $\nu_\mu \rightarrow \nu_\tau$  oscillations in the CNGS beam: Experimental proposal," CERN-SPSC-2000-028 (CERN, Geneva, 2000) [LNGS-P25-00].
2. N. Agafonova et al. (OPERA Collaboration), "Search for the  $\nu_\mu \rightarrow \nu_\tau$  oscillation with the OPERA hybrid detector," *Phys. Part. Nucl.* **44**, 703–727 (2013).
3. R. Acquafredda et al. (OPERA Collaboration), "The OPERA experiment in the CERN to Gran Sasso neutrino beam," *JINST* **4**, 04018 (2009).
4. Y. Fukuda et al. (Super-Kamiokande Collaboration), "Evidence for oscillation of atmospheric neutrinos," *Phys. Rev. Lett.* **81**, 1562 (1998).
5. L. Chaussard and G. Moret, "Vertex resolution and brick finding efficiency using scintillators information: Single charged particles simulation," OPERA Internal note, 28 March, 2000.
6. G. Moret et al., "Brick finding efficiency: Monte Carlo comparisons between several scintillating tracker options," OPERA Internal note, 23 May, 2001.
7. I. Laktineh, "Brick finding efficiency in muonic decay tau neutrino events", OPERA Internal note, 21 Jan., 2002.
8. I. Laktineh, "Brick finding efficiency of no-muon tau neutrino events in OPERA," OPERA Internal note, 18 Nov., 2002.
9. S. Dmitrievsky, Yu. Gornushkin, and G. Ososkov, "Neural networks, cellular automata, and robust approach applications for vertex localization in the OPERA Target Tracker detector", Preprint No. E10-2005-216 (Joint Institute for Nuclear Research, Dubna, 2005).
10. A. Chukanov, S. Dmitrievsky, and Yu. Gornushkin, "Neutrino interaction vertex location with the OPERA electronic detectors," OPERA public note no. 162, 2013.
11. T. Adam et al. (OPERA Collaboration), "The OPERA experiment Target Tracker," *Nucl. Instrum. Methods Phys. Res. A* **577**, 523 (2007).
12. A. Glazov, I. Kisel, E. Konotopskaya, and G. Ososkov, "Filtering tracks in discrete detectors using a cellular automaton," *Nucl. Instrum. Methods Phys. Res. A* **329**, 262—268 (1993).
13. R. Brun et al., "GEANT3," CERN-DD/EE/84-1 (1986).
14. P. V. C. Hough, "A method and means for recognizing complex patterns", US Patent No. 3069654 (Dec. 1962).
15. G. Ososkov, "Elastic arm methods of data analysis as a robust approach," *Tatra Mount. Math. Publ.* **26**, 291–306 (2003).
16. T. Khanna, *Foundation of Neural Networks* (Addison-Wesley, New York, 1989).
17. M. A. Branch, T. F. Coleman, and Y. Li, "A subspace, interior, and conjugate gradient method for large-scale bound-constrained minimization problems," *SIAM J. Sci. Comp.* **21** (1), 1–23 (1999).
18. A. Zell, G. Mamier, M. Vogt, and N. Mache, <http://www.ra.cs.uni-tuebingen.de/SNNS>, 1998.
19. Y. R. Quinlan, "Simplifying decision trees," *Int. J. Man-Mach. Stud.* **28**, 221 (1987).

*Translated by E. Kravchenko*